Neurosci Bull June 1, 2012, 28(3): 259–270. http://www.neurosci.cn
DOI: 10.1007/s12264-012-1243-5

·Original Article·

Characterization of amyloid-β precursor protein intracellular domain-associated transcriptional complexes in SH-SY5Y neurocytes

Wulin Yang[1], Amy Yong Chen Lau[2], Shuizhong Luo[1], Qian Zhu[3], Li Lu[3]

[1]*School of Biotechnology and Food Engineering, Hefei University of Technology, Hefei 230009, China*
[2]*Laboratory of Metabolic Medicine, Singapore Bioimaging Consortium (SBIC), Agency for Science, Technology and Research (A*STAR), Singapore*
[3]*Department of Anatomy, Shanxi Medical University, Taiyuan 030001, China*

Abstract: Objective Alzheimer's disease (AD) is one of the major disorders worldwide. Recent research suggests that the amyloid-β precursor protein intracellular domain (AICD) is a potential contributor to AD development and progression. The small AICD is rapidly degraded after processing from the full-length protein. The present study aimed to apply a highly efficient biotinylation approach *in vitro* to study AICD-associated complexes in neurocytes. **Methods** By co-expressing *Escherichia coli* biotin ligase with biotinyl-tagged AICD in the SH-SY5Y neuronal cell line, the effects of AICD overexpression on cell proliferation and apoptosis were analyzed. Besides, AICD-associated nuclear transcriptional complexes were purified and then examined by mass spectrometry. **Results** Our data showed that AICD overexpression not only affected cell proliferation but also led to apoptosis in differentiated SH-SY5Y cells. Moreover, biotinylation allowed single-step purification of biotinylated AICD-associated complexes from total nuclear extract via high-affinity biotin-streptavidin binding. Following this by mass spectrometry, we identified physically associated proteins, some reported previously and other novel binding partners, CUX1 and SPT5. **Conclusion** Based on these results, a map of the AICD-associated nuclear interactome was depicted. Specifically, AICD can activate CUX1 transcriptional activity, which may be associated with AICD-dependent neuronal cell death. This work helps to understand the AICD-associated biological events in AD progression and provides novel insights into the development of AD.

Keywords: Alzheimer's disease; amyloid-β precursor protein; AICD; biotinylation; apoptosis

1 Introduction

Alzheimer's disease (AD) is a slowly-progressing and adult-onset neurodegenerative disorder, affecting millions of people worldwide[1]. Affected individuals suffer from progressive loss of cognition and memory as well as language[1]. Studies are still under way to find effective therapeutics or drugs to prevent progression of the disease, in order to improve the quality of life of AD patients.

The pathological hallmarks of AD are significant accumulation of intracellular neurofibrillary tangles and deposition of extracellular senile plaques[1]. Neurofibrillary tangles contain hyper-phosphorylated tau, while senile plaques contain amyloid-β protein (Aβ). Both are toxic to synapses when in a soluble intermediate form[1-3], resulting

Corresponding authors: Wulin Yang, Li Lu
Tel: +65-64788728, +86-351-4135787; Fax: +65-64789957
E-mail: wulinyoung@163.com, yang_wulin@sbic.a-star.edu.sg, luli7300@126.com
Article ID: 1673-7067(2012)03-0259-12
Received date: 2011-12-16; Accepted date: 2012-03-08

in synaptic dysfunction and neurodegeneration, which account for the impairments of cognition and memory in AD patients.

Much work on AD has focused on understanding how Aβ contributes to the pathogenesis[4]. Aβ is a 38–43 amino-acid peptide derived from amyloid-β precursor protein (APP)[5], which is a type I transmembrane glycoprotein that can be processed via non-amyloidogenic and amyloidogenic pathways[6]. The non-amyloidogenic processing of APP involves sequential cleavage by α- and γ-secretases: APP is first cleaved by α-secretase to release a soluble ectodomain (APPsα) and a membrane-bound α-C-terminal fragment (α-CTF); the α-CTF is subsequently targeted by γ-secretase, which cleaves it within the transmembrane domain to simultaneously produce p3 (N-terminally truncated Aβ) and APP intracellular domain (AICD) fragments[5]. Since this pathway precludes Aβ production, it is termed non-amyloidogenic. On the other hand, amyloidogenic processing of APP involves β- and γ-secretases: the β-secretase first cleaves APP to generate a soluble ectodomain (APPsβ) and β-CTF; β-CTF is then cleaved by γ-secretase to produce Aβ and AICD[6]. A transcriptionally active complex of AICD is associated with Fe65 and histone acetyltransferase Tip60[5]. The γ-secretase can cleave the CTF of APP at different sites, generating different isoforms of Aβ and AICD[7]. For example, cleavage at the valine residue at position 636 (V636) releases $A\beta_{40}$ and $AICD_{59}$, the commonly secreted products. Alternatively, cleavage at the ε-cleavage site generates the $AICD_{50}$ isoform[7].

Notably, both amyloidogenic and non-amyloidogenic processing of APP produce a 6-kDa AICD fragment. Unlike Aβ that is released from cells, AICD is retained in the cytoplasm. Therefore, AICD is proposed to have a more direct or an earlier impact on AD pathology than the extracellular Aβ[7]. Failure of effective Aβ-targeted therapies against AD also supports the proposition that Aβ is not the only factor that causes the disease[8].

Numerous *in vivo* studies using transgenic mice have demonstrated a possible role of AICD in AD pathogenesis. Recent work by Ghosal *et al.*[2] indicated that AICD is an Aβ-independent factor that contributes to AD. They found that transgenic mice expressing $AICD_{59}$ exhibit high levels of active glycogen synthase kinase-3β (GSK3β), which leads to hyper-phosphorylation of tau. As hyper-phosphorylated tau protein begins to aggregate, deficiency in memory becomes apparent. These phenomena in $AICD_{59}$-transgenic mice are often typical in human AD brain. Another study[9] assessed synaptic transmission and learning deficits in transgenic mice that over-express an AICD isoform of 31 amino-acids ($AICD_{31}$). The $AICD_{31}$ is released upon caspase cleavage of APP at the lysine residue at position 664 (D664). The presence of $AICD_{31}$ in the cytoplasm induces DNA fragmentation and caspase-3 activation in neurons[7], which might explain the observed dysfunctions of synaptic transmission and learning in these $AICD_{31}$ transgenic mice. A single amino-acid mutation at D664 precludes γ-secretase cleavage and $AICD_{31}$ production. These mutant transgenic mice lacking $AICD_{31}$ are protected from the loss of synaptic plasticity and transmission as well as learning. Both studies demonstrated the potential importance of AICD in AD progression and development.

The ability of AICD to activate genes and induce cellular processes is proposed to be attributed to its transactivation function. AICD released intracellularly can form functional complexes with different proteins, translocate into the nucleus, initiate signal transduction and activate the transcription of target genes[3,10]. Over twenty proteins have been reported to interact with AICD[7]. For example, AICD associates with APP adaptor protein, Fe65 and the Fe65-binding nuclear histone acetylase, Tip60, to form the functional AICD-Fe65-Tip60 complex[6], which induces the transcription of target genes such as *APP* and *GSK3β*[11]. On the other hand, AICD-Mint3-TAZ and AICD-Mint3-YAP are recently uncovered novel mediators of APP signaling[12]. These discoveries provide the insight that AICD may contribute to AD pathogenesis by forming protein complexes to induce the transactivation of gene expression, which eventually leads to disease progression. The AICD-Fe65-Tip60 transcriptional complex was identified using an artificial system[6]. However, such a system might not reveal the actual biological events occurring in the nuclei of neurons. Hence, the existence of the identified

binding partners for AICD in neurons remains questionable, and needs to be clarified.

Biotinylation is an efficient approach to isolate and purify biotinyl-tagged protein from crude nuclear extract *in vivo* and *in vitro*[13]. Using a similar biotinylation approach, we aimed to isolate AICD-associated complex(es) in a single step by subjecting total nuclear extracts to streptavidin bead binding, to further understand the role of AICD-related pathways in AD progression.

2 Materials and methods

2.1 Cell culture The SH-SY5Y human neuroblastoma cell line was cultured in minimum essential medium/F12 Kaighn's medium (MEM/F12K) (Invitrogen, Carlsbad, CA) supplemented with 10% fetal bovine serum (FBS) and antibiotics (penicillin/streptomycin). The HEK 293TN cell line was cultured in Dulbecco's modified Eagle's medium (Invitrogen) supplemented with 10% FBS and antibiotics. Both cell lines were incubated at 37°C with 5% CO_2, and the culture media were changed every two days. For seeding cells, the old culture medium was aspirated, and trypsin was added to detach cells from the dish surface. Subsequently, appropriate fresh culture medium was added to neutralize the trypsin. Re-seeded cells were allowed to grow up to 50%–70% confluence for transfection and infection.

2.2 Constructs The *Escherichia coli* biotin-protein ligase gene (BirA) and a V5 sequence were cloned into the BamHI site of pEFα vector, which was kindly provided by Prof. Stuart H. Orkin (Harvard Medical School), to generate the L309-BirA/V5-His construct. The BirA gene fragment and its downstream V5 tag were cut from pEFα-BirA/V5-His and sub-cloned into lentiviral vector L309 (a kind gift from Dr. Zhiping Pang, Stanford University) at the BamHI site. $AICD_{50}$ and $AICD_{59}$ were first constructed in pEFα vector fused with a biotin tag at the N-terminus, and then transferred to lentivector L309. cDNAs of mouse Cux1 and SPT5 constructs were obtained by reverse transcription and cloned into pCMV5-myc vector to generate myc-tagged proteins. MKLP1 promoter constructs were obtained by cloning PCR-amplified promoter regions into the PGL-3 basic Luc reporter plasmid as previously reported[14].

2.3 Pseudovirus production and infection The 293TN cells were used as virus-producer cells. For packaging of pseudoviral particles, the BirA and AICD expression constructs, combined with packaging plasmids (Gag-Pol, Rev and Envelope proteins) were co-transfected into 293TN cells according to the protocols in the Effectene Transfection Reagent Handbook (QIAGEN, Hilden, Germany). Transfected cells were allowed to grow for at least two days, and the culture medium containing pseudoviral particles was collected, filtered, and added into SH-SY5Y cell cultures. The SH-SY5Y cells were infected with BirA-packaged pseudovirus. After two days, they were infected with AICD-packaged pseudoviruses.

2.4 Bromodeoxyuridine (BrdU) incorporation assay, caspase-3/7 activity assay and dead cells counting To assess cell proliferation, the cells were labeled with BrdU (10 μmol/L) (Calbiochem, San Diego, CA) for 1 or 2 days, then fixed in PBS with 4% paraformaldehyde at room temperature for 20 min. After DNA denaturation in 2 N HCl, cells were permeabilized with 0.1% Triton X-100 in PBS, and treated with serum to block nonspecific binding. The cells were incubated with mouse anti-BrdU (Calbiochem) overnight at 4°C, stained with cy3-labeled goat anti-mouse antibody for 1 h at 37°C, and then mounted using Vectashield mounting medium for fluorescence staining with 4',6-diamidino-2-phenylindole (DAPI) (Vector Laboratories, Burlingame, CA). BrdU-positive ($BrdU^+$, cy3-labeled) cells and total cells (nuclei stained by DAPI) were quantified in at least 10 sections.

The caspase-3/7 assay was performed according to the protocols provided by Promega (Madison, WI). Briefly, cells stably expressing $AICD_{50/59}$ and control cells were treated with retinoic acid (RA) for 4 days. Then they were collected and lysed with 1× reporter lysis buffer. Cell lysates and caspase-3/7 substrate Z-DEVD-R110 were mixed and incubated at 37°C for 1 h. Fluorescence was measured on a fluorescence reader (Bio-Tek synergy HT, Winooski, VT). Reporter lysis buffer without lysate was used to measure background fluorescence.

To determine the quantity of dead cells, $AICD_{59}$, $AICD_{50}$ and control cells were plated at a density of 2 × 10^5 cells per well in a 12-well dish. After treatment with RA (on day 2 after plating) to induce differentiation for another 2 or 4 days, dead cells were stained with trypan blue and counted using a hemocytometer.

2.5 Real-time quantitative PCR (qPCR) Total RNA was isolated from cultured cells with TRIzol (Invitrogen) at appropriate time points and reverse transcribed using SuperScript II reverse transcriptase and random primers (Fermentas, Hanover, MD). Real-time qPCR was performed on a StepOnePlus™ Real-Time PCR System (Applied Biosystems, Foster City, CA) using the SYBR® Green PCR Master Mix reagent kit (Applied Biosystems). Expression level of TATA-box binding protein (TBP) was used as an internal control. The primers were as follows: Cyclin A forward: 5'-GAGAGGGAAATTGCAGCTTG-3', reverse: 5'-CGGGCGGATATATCTCTTCA-3'; Cyclin B forward: 5'-ATGGTGCATTTTGCTCCTTC-3', reverse: 5'-TCCATTCACCGTTGTCAAGA-3'; Cyclin E forward: 5'-CCTCCAAAGTTGCACCAGTT-3', reverse: 5'-CCACTTAAGGGCCTTCATCA-3'; CDK1 forward: 5'-AGCTCTGGGCACTCCTAACA-3', reverse: 5'-TCCACTTGGGAAAGGTGTTC-3'; CDK2 forward: 5'-ATGGACGGAGCTTGTTATCG-3', reverse: 5'-CATC CTGGAAGAAAGGGTGA-3'; TBP forward: 5'-ACCCT TCACCAATGACTCCTATG-3', reverse: 5'-TGACTG CAGCAAATCGCTTGG-3'.

2.6 Nuclear extract preparation Nuclear extracts were prepared according to procedures described previously[13]. Both groups of cells were harvested by centrifugation at 640 *g* and washed once with cold PBS. The cell pellet was resuspended in 2.2 mol/L sucrose in 10 mmol/L Hepes, pH 7.5, 25 mmol/L KCl, 0.15 mmol/L spermine (Sigma-Aldrich, St. Louis, MO), 0.5 mmol/L spermidine (Sigma-Aldrich) and 1 mmol/L EDTA and incubated for 20 min. Subsequently, cells were lysed and lysis was checked under a light microscope by nuclear staining with methyl green-pyronin (Sigma-Aldrich). Nuclei were pelleted by ultracentrifugation at 141 000 *g* for 2 h at 4°C. The pellet was resuspended in lysis buffer (containing in mmol/L: 10 Hepes, pH 7.5, 200 KCl, 3 $MgCl_2$, 0.1 EDTA, and 20% glycerol). Nuclei were extracted by drop-wise addition of 3.3 mol/L KCl until the final concentration was ~400 mmol/L. Insoluble material was then removed by ultracentrifugation at 300 000 *g* for 1 h at 4°C. Nuclear extracts were aliquoted and stored at -70°C.

2.7 Streptavidin binding assay The streptavidin binding assay was performed according to a previous report[13]. Streptavidin magnetic beads (New England Biolabs, Hertfordshire, UK) were blocked by three washes in TBS with 200 ng/μL bovine serum albumin (Sigma-Aldrich). Beads were used at 40 μL/2 mg total nuclear extract. Binding was performed in 1× TBS, 350 mmol/L NaCl, and 0.3% Nonidet P-40 at 4°C overnight on a rocking platform. Protease inhibitor cocktail (Santa Cruz, Heidelberg, Germany) was added to the binding solution. After overnight binding, beads were washed six times in binding solution. Beads were centrifuged at 5 000 r/min for 2 min at 4°C after each wash. Bound material was eluted by boiling for 5 min in Laemmli buffer.

2.8 Western blot Harvested cells were lysed by adding Laemmli buffer and heated at 100°C for 5–10 min for protein expression and biotinylation analysis of BirA, $AICD_{59}$, and $AICD_{50}$. Samples were resolved in 10%–20% Tris-Tricine Ready Gel (Bio-Rad, Hercules, CA) in 1× Tris, Tricine and SDS buffer, and transferred onto nitrocellulose membranes using an iBlot™ Device with Blotting Roller (Invitrogen). The membrane was blocked in 5% non-fat dry milk (Bio-Rad) supplemented with sodium azide for 1 h at room temperature. Thereafter, the membrane was incubated with mouse anti-FLAG monoclonal antibody (1:1 000, Sigma-Aldrich), streptavidin-horseradish peroxidase (HRP) conjugate (1:5 000, Abcam, Cambridge, MA) or rabbit anti-caspase-3/7 antibody (1:1 000; Cell Signaling, Beverley, MA) for 1 h at room temperature. After three washes with PBST (PBS with 0.1% Tween 20) for 10 min, the membrane was incubated with secondary anti-mouse or anti-rabbit antibody (1:10 000; GE Healthcare, Chalfont, UK) for 1 h, and again washed three times with PBST. Finally, the membrane was incubated with detection solution using electrochemiluminescence (ECL) with an ECL

Advance™ Western blotting detection kit (GE Healthcare) for 5 min. Western blots were developed using a Kodak medical X-ray processor (Carestream Health, Rochester, NY).

2.9 Immunostaining Cells cultured on coverslips were rinsed three times in 1× PBS, and fixed in 400 μL 4% paraformaldehyde for 20 min at room temperature, followed by five washes in PBS and 0.1% Triton-X 100 and five rinses with PBS. Then cells were blocked with 10% normal goat serum (Invitrogen) in PBS for 1 h, incubated with primary mouse anti-FLAG antibody (1:50; Sigma-Aldrich) at room temperature overnight, washed thrice with PBS and incubated with Alexa Fluor 488 donkey anti-mouse antibody (1:200; Invitrogen). The coverslips were subsequently dried and mounted onto glass slides with mounting medium containing DAPI. Cells were then examined using a confocal microscope (Nikon Imaging Centre, Singapore Bioimaging Consortium, Singapore).

2.10 Silver staining Protein complex(es) eluted from streptavidin beads were resolved by 12% SDS-PAGE and then fixed in 50% methanol with 10% acetic acid for 1 h. Subsequently, the gel was washed with sterile water (ddH_2O) for at least 5 min, and then treated with 30% ethanol for 20 min. Proteins then underwent sensitization with 0.02% sodium thiosulfate for 1 min, were rinsed with ddH_2O for 60 s, impregnated with silver nitrate for 20 min, and washed three times in ddH_2O. Color was developed in a solution of 3% sodium carbonate, 0.05% formaldehyde and 0.0005% sodium thiosulfate. Residual developing reagent was washed away with ddH_2O. Development was stopped by incubation with 1.4% sodium-EDTA for 5 min. Finally, the gel was rinsed thrice with ddH_2O prior to densitometry (Bio-Rad).

2.11 Mass spectrometry (MS) Visible bands were excised from the gel, subjected to reduction with 25 mmol/L dithiothrietol at 56°C and alkylation with 55 mmol/L indole-3-acetic acid at room temperature, followed by in-gel digestion with MS-grade trypsin (Promega) 10 ng/μL in 25 mmol/L ammonium bicarbonate buffer, pH 8.0 for 16 h at 37°C. Peptides were extracted and spotted onto matrix-assisted laser desorption/ionization (MADLI) target plates with HCCA (α-cyano-4-hydroxy-cinamic acid) as matrix. MALDI-time-of-flight (TOF)-TOF MS/MS was carried out at Bruker Ultraflex III TOF-TOF with the support of the softwares FlexControl 3.0, FlexAnalysis 3.0 and Biotools 3.2. Mass lists were submitted to an in-house Mascot server for database search, which was assisted by the Laboratory of Bioimaging Probe Development, Singapore Bioimaging Consortium.

2.12 Co-immunoprecipitation 293TN cells were co-transfected with plasmids expressing FLAG-tagged $AICD_{50}$ and myc-tagged CUX1 or SPT5. Two days after transfection, total lysates were prepared and incubated with anti-FLAG antibody for 4 h. Then protein-A agarose beads were added. After 2 h, unbound material was washed away with lysis buffer. Bound material was boiled in Laemmli buffer and subjected to Western blot with anti-myc antibody (Santa Cruz).

2.13 Luciferase assay The SH-SY5Y cells were cultured in MEM/F12K supplemented with 10% FBS and antibiotics (penicillin/streptomycin) in a 37°C incubator with 5% CO_2. One day after plating, co-transfection of SH-SY5Y cells with relevant DNA constructs was performed by electroporation using Gene Pulser (Bio-Rad). Forty-eight hours later, the cells were washed with PBS and lysed in 200 μL of 1× passive lysis buffer included in the dual luciferase reporter assay system (Promega). Luciferase activity was measured in cell extracts on a luminometer (Molecular Devices, Sunnyvale, CA). The firefly luciferase activity was normalized to *Renilla* luciferase activity.

2.14 Statistical analysis Comparisons were made using the two-tailed Student's *t*-test with equal variance. $P < 0.05$ was indicated as statistically significant.

3 Results

3.1 Biotinylation of $AICD_{50/59}$ in 293TN and SH-SY5Y cells The L309-BirA-IRES-EGFP construct contained BirA biotin ligase that biotinylates the biotinyl (BIO) sequence present in the AICD expression constructs. Biotinylation should only be detected in BirA/$AICD_{50/59}$ co-transfected 293TN and infected SH-SY5Y cells. To determine if BIO-tagged $AICD_{50/59}$ were expressed in these cells, we performed Western blot using streptavidin-HRP conjugate, since it binds to biotinylated proteins with high

affinity. Biotinylation was detectable only in those 293TN cells that expressed both BirA and AICDs constructs, and no biotinylation of BIO-tagged $AICD_{50/59}$ was detected in the absence of BirA (Fig. 1A).

The packaged pseudo-lentiviral particles containing the BirA, $AICD_{50}$ or $AICD_{59}$ expression constructs, released from 293TN producer cells, were used to infect SH-SY5Y cells. Western blot results showed that biotinylation of BIO-tagged $AICD_{59}$ and $AICD_{50}$ in the SH-SY5Y cells was only detectable in those co-infected with lentiviral particles containing BirA expression constructs (Fig. 1B). However, the band for biotinylated $AICD_{59}$ was very faint compared to $AICD_{50}$, probably because $AICD_{59}$ can be further cleaved by γ-secretase to release the $AICD_{50}$ frag-

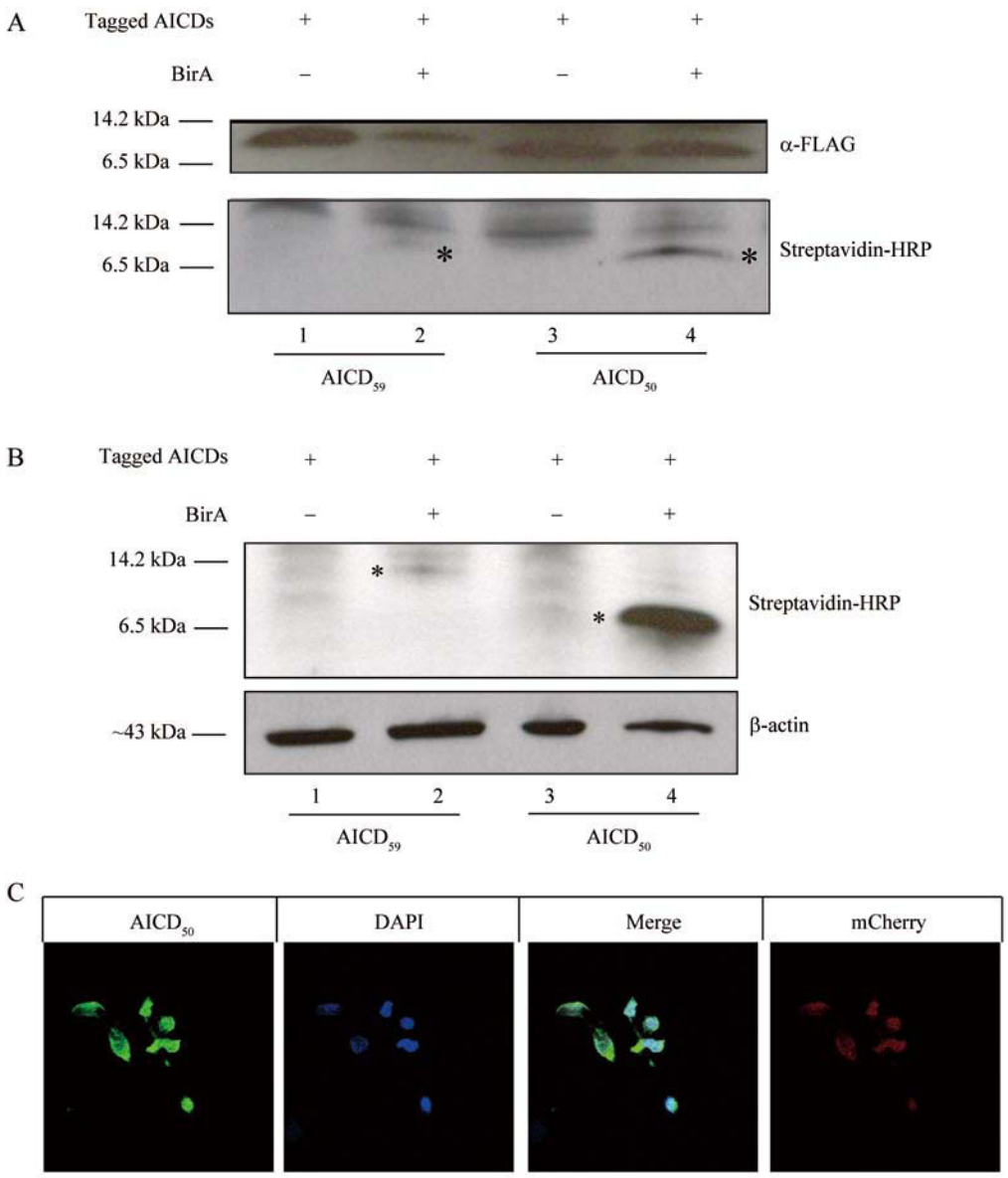

Fig. 1. Biotinylation of amyloid-β precursor protein intracellular domain $AICD_{59/50}$ by co-expressed biotinylation ligase BirA. A and B: Western blots showing biotinylation of biotinyl-tagged $AICD_{59}$ and $AICD_{50}$ in transfected 293TN cells (A) and SH-SY5Y cells (B). Asterisks indicate specific biotinylation of biotinyl-tagged $AICD_{59/50}$. C: Localization of $AICD_{50}$ in SH-SY5Y cells determined by immunostaining.

ment. In this way, the N-terminal-fused BIO-tag would be removed from $AICD_{59}$. Thus, in the following experiments, we focused on analysis of $AICD_{50}$ instead of $AICD_{59}$.

3.2 Localization of $AICD_{50}$ in SH-SY5Y cells Localization of $AICD_{50}$ in SH-SY5Y cells was observed using confocal microscopy. The nuclei were stained blue by DAPI, while the FLAG-tagged $AICD_{50}$ was stained green. The expression of L309-$AICD_{50}$-IRES-mCherry constructs in SH-SY5Y cells was shown as red fluorescence, due to the mCherry marker. The merged image revealed that $AICD_{50}$ was located in both the nucleus and cytoplasm, predominantly in the nucleus (Fig. 1C).

3.3 $AICD_{50/59}$-expressing cells show reduced proliferation Since cells expressing $AICD_{50/59}$ grow slower than control cells, we measured cell proliferation by BrdU assay. Freshly infected cells were incubated with BrdU for 1 or 2 days, fixed, and stained with anti-BrdU antibody. $BrdU^+$ cells were counted in at least 10 sections. Compared to control cells, the number of $BrdU^+$ cells was dramatically decreased in those expressing $AICD_{59}$ or $AICD_{50}$ (Fig. 2A). Also, we used another cell line, neuron-2a (N2a), to investigate the effect of AICD on cell proliferation and similar results were obtained (Fig. S1A). These results indicated that AICD can cause deficits in cell proliferation in SH-SY5Y cells. Next, we assessed the expression of genes related to the cell cycle and found that the expression of cyclins A, B, and E and the corresponding CDKs 1 and 2 were down-regulated in the AICD-expressing cells (Fig. 2B), suggesting that AICD directly or indirectly regulates the cell cycle at the transcriptional level.

3.4 AICD overexpression induces apoptosis in differentiated SH-SY5Y cells Although overexpression of AICD

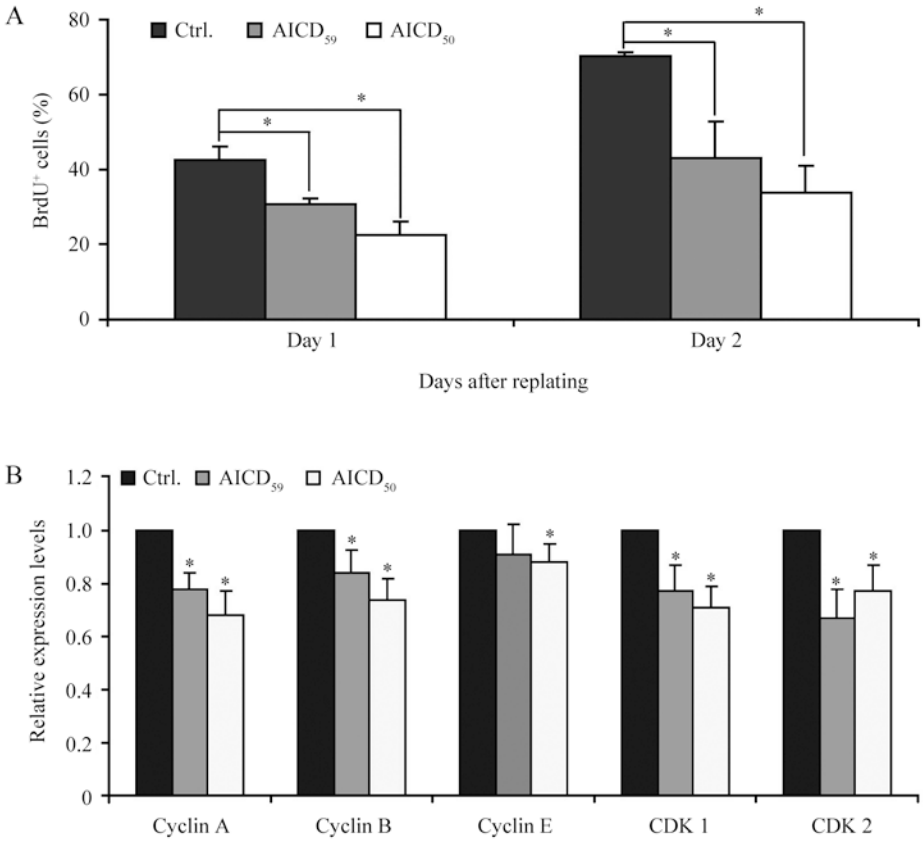

Fig. 2. Amyloid-β precursor protein intracellular domain (AICD)-overexpressing cells show decreased proliferation. A: BrdU incorporation assay showing significantly fewer BrdU-labeled cells in AICD-expressing cells than in control cells (Ctrl.). B: Real-time PCR analyses showing that cell cycle-related genes were down-regulated in AICD-expressing cells. Data are presented as mean ± SE and are from at least three independent experiments. *P <0.05 *vs* control.

reduced cell proliferation, cells did not exhibit apparent cell death (data not shown). Previous work suggested that AICD forms a transcriptional complex with Fe65 and Tip60 to promote apoptosis. We thus supposed that AICD may induce cell apoptosis during neurogenesis. Here, RA was used to promote neurogenesis in SH-SY5Y cells. To determine the quantity of dead cells, $AICD_{59}$, $AICD_{50}$ and control cells were plated at a density of 2×10^5 cells per

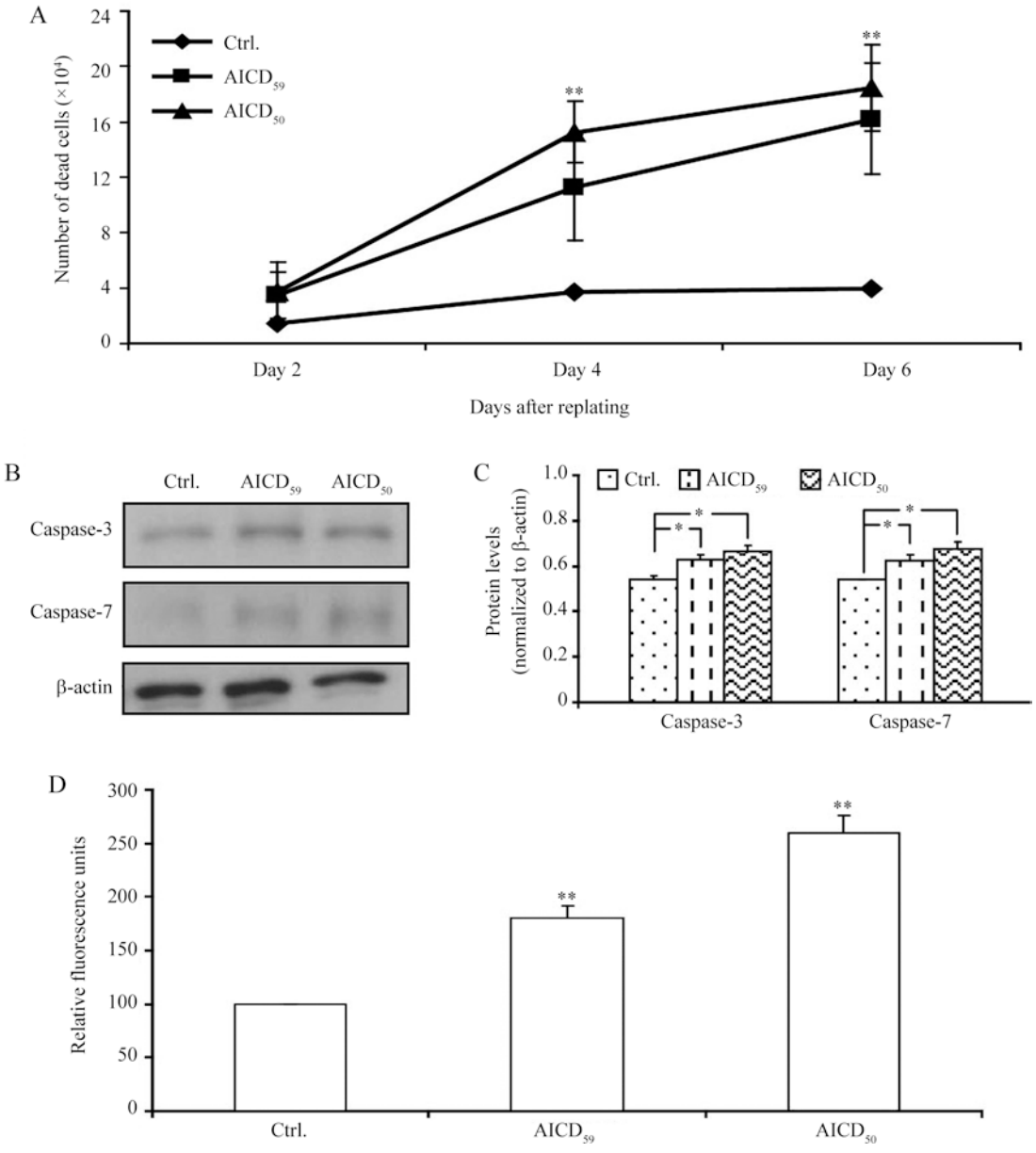

Fig. 3. Amyloid-β precursor protein intracellular domian (AICD) induces apoptosis in differentiated SH-SY5Y cells. A: The number of dead cells was counted by trypan blue staining before, and on days 2 and 4 after retinoic acid treatment (that is, on days 2, 4 and 6 after plating). The number of dead cells was significantly increased in the AICD group compared to the control group (Ctrl.). Data are presented as mean ± SE. $n = 4$. $^{**}P < 0.01$. B: Representative Western blots for caspase-3 and caspase-7 showing they were up-regulated in AICD-expressing cells. C: Relative levels of proteins quantified using ImageJ and normalized to actin levels. Data are presented as mean ± SE. $n = 3$ in each group. $^{*}P < 0.05$. D: Caspase-3 activity measured using fluorescence assay. Relative fluorescence units were increased in AICD-overexpressing cells. Data are presented as mean ± SE. $n = 4$. $^{**}P < 0.01$.

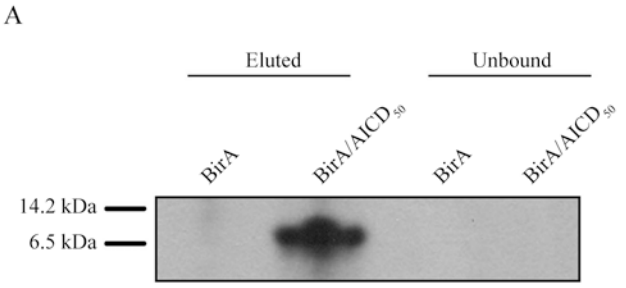

B

Protein ID	Peptides Nos
Fe65	5
MED12	2
Numb	1
SET	6
Fe65L1	3
Fe65L2	1
SPT5	1
CUX1	1

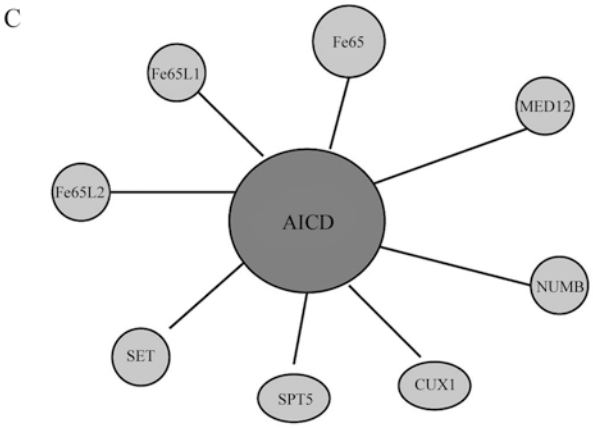

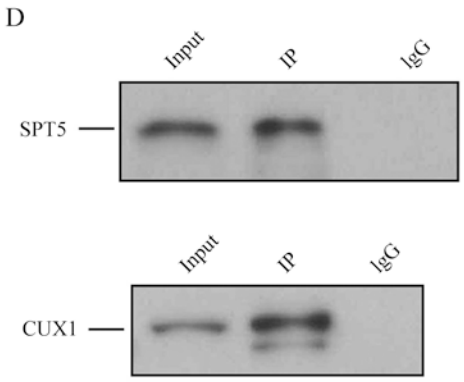

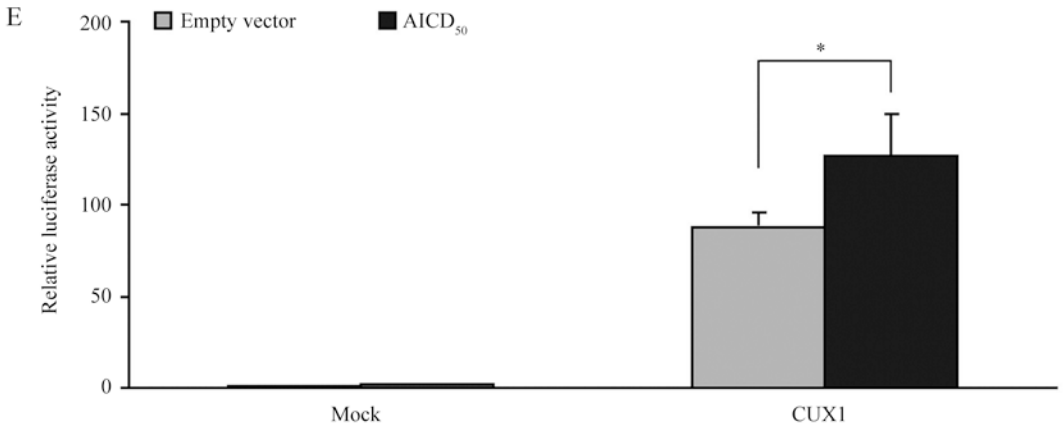

Fig. 4. $AICD_{50}$-associated nuclear complexes. A: Western blot showing binding efficiency of biotinylated $AICD_{50}$ (BirA/$AICD_{50}$) to streptavidin beads. B: Proteins specifically co-purifying with biotin-tagged $AICD_{50}$ compared to control purification by mass spectrometry. Protein ID, Protein identity; Peptide Nos, numbers of peptides identified for each protein. C: A model for AICD-associated nuclear protein complexes. D: Immunoprecipitation (IP) was used to confirm the interaction of AICD with two novel molecules, SPT5 and CUX1. E: Luciferase assay was used to assess the effect of AICD on the activity of CUX1-drived MKLP1 promoter activity. CUX1 activated MKLP1 promoter activity compared to the Mock group (without CUX1-expressing plasmid). $AICD_{50}$ enhanced this luciferase activity by co-transfection of $AICD_{50}$- and CUX1-expressing plasmids. Data (mean ± SE) are from at least three independent experiments. *P <0.05.

well in a 12-well dish. After treatment with RA (on day 2 after plating) to induce differentiation for another 2 or 4 days, dead cells were stained with trypan blue and counted using a hemocytometer. The numbers of dead cells with $AICD_{59}$ or $AICD_{50}$ overexpression were significantly increased (Fig. 3A). The same results were found in N2a cells (Fig. S1B). The apoptosis markers, caspase-3 and caspase-7, were checked after RA treatment. Both were up-regulated in the $AICD_{50/59}$-expressing cells compared with the control cells (Fig. 3B, C). Further, caspase-3/7 enzyme activity was assessed under the same conditions. Enzyme activity was dramatically increased in AICD-stable cells (Fig. 3D). All these results suggest that AICD induces apoptosis in differentiated SH-SY5Y cells by activating caspase-3/7 activity.

3.5 Characterization of AICD-associated transcriptional complexes As indicated above, AICD may act as a functional signaling molecule to modulate the activity of neurocytes at the transcriptional level. Thus, our aim was to determine the partners associated with AICD at the transcriptional level. Due to the low level of biotinylated $AICD_{59}$, only the crude extracts of BirA/$AICD_{50}$-infected SH-SY5Y cells were subjected to streptavidin pull-down assay. Both the bound and flow-through fractions from the beads were collected for biotinylation efficiency analysis. The efficiency of biotinylated $AICD_{50}$ binding to the streptavidin beads was tested by Western blot using streptavidin-HRP conjugate.

A strong band corresponding to the biotinylated $AICD_{50}$ in the eluted fraction was found (Fig. 4A). Conversely, biotinylation was absent from the unbound fraction. Background binding was also negligible due to the absence of a biotinylated band in the BirA control.

Since the BIO-tagged $AICD_{50}$ was efficiently recovered from the eluted fraction after streptavidin bead binding, the protein complexes associated with BIO-tagged $AICD_{50}$ should also be found only in the eluted fraction. By comparing the bands recovered from the eluted fractions of BirA control and BirA/$AICD_{50}$, several distinct bands were found for biotinylated $AICD_{50}$ (BirA/$AICD_{50}$) (Fig. S2). These bands might correspond to the purified BIO-tagged $AICD_{50}$-associated protein complexes, so they were excised for tandem MS-MS analysis. Results showed that the proteins were associated with $AICD_{50}$ (Fig. 4B, C), and may cooperate in AICD-related transcriptional activity. Fe65, an important AICD binding partner[6], was confirmed in this work, as well as its two homologs, Fe65L1 and Fe65L2. Some other previously suggested binding partners were also detected: SET[15], MED12[16], and Numb[17]. Importantly, we found two transcription factors, CUX1 and SPT5, as novel AICD binding partners. Their interactions with $AICD_{50}$ were confirmed by co-immunoprecipitation assay (Fig. 4D). Moreover, AICD enhanced the activity of CUX1-dependent activation of the MKLP1 promoter (Fig. 4E). These results suggested that AICD modulates cell proliferation and apoptosis through different pathways, besides the canonical Fe65-dependent pathway.

4 Discussion

The present study aimed to reveal AICD-associated binding partners in SH-SY5Y cells by using the biotinylation approach. The small-molecule AICDs are unstable in cells and are often rapidly degraded upon release[3], making their study difficult. To overcome this, we used an over-expression system by cloning an AICD gene fragment into L309 lentiviral vector. The biggest advantages of delivering target genes into target cells using lentiviral vector are stability and the continuous expression of the genes. The streptavidin pull-down assay and MS allowed the identification of AICD-associated transcriptional complexes in SH-SY5Y cells. Besides known binding partners, such as Fe65, two novel components, CUX1 and SPT5, were found in this work. AICD may modulate cell activity via different binding partners. This work helps to elucidate AICD-associated cellular events and the relationship between AD pathology and AICD-derived signal transduction.

Biotin has an extremely strong affinity for streptavidin, with a dissociation constant between 10^{-13} and 10^{-15} mol/L[13]. Hence, biotin-streptavidin binding allows highly efficient purification of biotinylated proteins as well as their associated complexes from crude extracts. Indeed, our

data revealed efficient binding of biotinylated $AICD_{50}$ to streptavidin beads in relation to the negligible background binding in BirA controls of both eluted and unbound materials from the beads. In addition, the protein complexes associated with $AICD_{50}$ were purified from nuclear extracts in just a single step. Our study revealed both nuclear and cytoplasmic localizations of AICD in SH-SY5Y cells, supporting the idea that intracellularly-released AICD can translocate into the nucleus. Many studies revealed that translocation of AICD into the nucleus is dependent on the Fe65 adaptor protein[3,6,18], while others showed that nuclear translocation of AICD may be indirectly through Fe65[2]. Our work confirmed that AICD is associated with Fe65 in the nucleus, indicating an Fe65-dependent translocation.

The slow growth observed in $AICD_{59}$ and $AICD_{50}$ stable SH-SY5Y cells was due to reduced rates of cell proliferation. This phenomenon has been neglected in previous work, much of which emphasized the apoptotic activity of AICD. The reduced cell proliferation may be due to the fact that AICD activates p53, which then regulates the cell cycle check point. Another possibility is that other AICD binding partners also function in this process. The two novel binding partners found in this study, CUX1 and SPT5, may participate, because they have been found to play broad roles in mammalian development by regulating gene expression and function in controlling cell proliferation[19,20].

It would be of interest to investigate the extent of apoptosis mediated by the intracellular domains, since this may be an important contributor to AD pathology. Cell death signals such as GSK3β, p53 and caspase activation transmitted by an AICD-dependent transcriptionally active complex have been reported[2,7]. For instance, $AICD_{31}$ induces DNA fragmentation and caspase-3 activation[7]. Besides, another study has reported a reduction of β-catenin level in $AICD_{59}$-expressing rat primary neurons[11]. A low β-catenin level can cause the loss of cell-cell contact and make neurocytes more vulnerable to apoptosis[7,21]. Here, we confirmed that AICD activates caspase-3/7 activity and found that AICD could activate CUX1-dependent activity, a potential add-on for AICD-dependent neuronal cell death. We hypothesize that AICD may be associated with different sets of proteins or molecules to control the molecular pathways of apoptosis.

The efficient and specific *in vitro* biotinylation method revealed the transcriptional complexes associated with $AICD_{50}$ in SH-SY5Y neurocytes. Combined with the use of MS, the components of these transcriptional complexes were identified. This provides a good basis for future functional studies to understand the relationship of AICD-transcriptional complexes with the corresponding pathways such as cell proliferation and apoptosis. Thus, a more comprehensive understanding of AICD- and APP-like protein intracellular domain-dependent AD pathological progression, can be reached. Hypothetically, the intracellular domains of the APP family may play multiple roles in the progression of AD. Therefore, future studies can investigate the molecular mechanism of AICD-mediated AD pathology by comprehensively elucidating the physiological and pathological AICD-associated transcriptional complexes, especially the two novel binding partners, CUX1 and SPT5. Further comprehensive studies are required to fully understand APP- and AICD-related biological processes, which may not only be helpful in understanding AD pathogenesis, but also provide new therapeutic targets against AD.

Supplemental Data: Supplemental Data include two figures and can be found online at http://www.neurosci.cn/epData.asp?id=20.

Acknowledgements: We thank Prof. Stuart H. Orkin (Harvard Medical School, Boston, MA) for providing BIRA plasmid and PEFα vector. This work was supported by grants from the National Natural Science Foundation of China (30800178, 30973094) and the Natural Science Foundation for Young Scientists of Shanxi Province, China (2009021045).

References:

[1] Sisodia SS, St George-Hyslop PH. γ-Secretase, notch, Aβ and Alzheimer's disease: Where do the presenilins fit in? Nat Rev

Neurosci 2002, 3: 281–290.

[2] Ghosal K, Vogt DL, Liang M, Shen Y, Lamb BT, Pimplikar SW. Alzheimer's disease-like pathological features in transgenic mice expressing the APP intracellular domain. Proc Natl Acad Sci U S A 2009, 106: 18367–18372.

[3] von Rotz RC, Kohli BM, Bosset J, Meier M, Suzuki T, Nitsch RM, *et al*. The APP intracellular domain forms nuclear multiprotein complexes and regulates the transcription of its own precursor. J Cell Sci 2004, 117: 4435–4448.

[4] Hardy J, Selkoe DJ. The amyloid hypothesis of Alzheimer's disease: Progress and problems on the road to therapeutics. Science 2002, 297: 353–356.

[5] Thinakaran G, Koo EH. Amyloid precursor protein trafficking, processing and function. J Biol Chem 2008, 283: 29615–29619.

[6] Cao X, Südhof TC. A transcriptionally active complex of APP with Fe65 and histone acetyltransferase Tip60. Science 2001, 293: 115–120.

[7] Muller T, Meyer HE, Egensperger R, Marcus K. The amyloid precursor protein intracellular domain (AICD) as modulator of gene expression, apoptosis, and cytoskeletal dynamics - relevance for Alzheimer's disease. Prog Neurobiol 2008, 85: 393–406.

[8] Pimplikar SW. Reassessing the amyloid cascade hypothesis of Alzheimer's disease. Int J Biochem Cell Biol 2009, 41: 1261–1268.

[9] Saganich MJ, Schroeder BE, Galvan V, Bredesen DE, Koo EH, Heinemann SF. Deficits in synaptic transmission and learning in amyloid precursor protein (APP) transgenic mice require C-terminal cleavage of APP. J Neurosci 2006, 26: 13428–13436.

[10] Slomnicki LP, Lesniak W. A putative role of the amyloid precursor protein intracellular domain (AICD) in transcription. Acta Neurobiol Exp (Wars) 2008, 68: 219–228.

[11] Kim HS, Kim EM, Lee JP, Park CH, Kim S, Seo Jh, *et al*. C-Terminal fragments of amyloid precursor protein exert neurotoxicity by inducing glycogen synthase kinase-3beta expression. FASEB J 2003, 17: 1951–1953.

[12] Swistowski A, Zhang Q, Orcholski ME, Crippen D, Vitelli C, Kurakin A, *et al*. Novel mediators of amyloid precursor protein signaling. J Neurosci 2009, 29: 15703–15712.

[13] Boer Ed, Rodriguez P, Bonte E, Krijgsveld J, Katsantoni E, Heck A, *et al.* Efficient biotinylation and single-step purification of tagged transcriptional factors in mammalian cells and transgenic mice. Proc Natl Acad Sci U S A 2003, 100: 7480–7485.

[14] Paul BM, Vassmer D, Taylor A, Magenheimer L, Carlton CG, Piontek KB, *et al.* Ectopic expression of Cux1 is associated with reduced p27 expression and increased apoptosis during late stage cyst progression upon inactivation of Pkd1 in collecting ducts. Dev Dyn 2011, 240: 1493–1501.

[15] Madeira A, Pommet JM, Prochiantz A, Allinquant B. SET protein (TAF1beta, I2PP2A) is involved in neuronal apoptosis induced by an amyloid precursor protein cytoplasmic subdomain. FASEB J 2005, 19: 1905–1907.

[16] Xu X, Zhou H, Boyer TG. Mediator is a transducer of amyloid-precursor-protein-dependent nuclear signalling. EMBO Rep 2011, 12: 216–222.

[17] Roncarati R, Sestan N, Scheinfeld MH, Berechid BE, Lopez PA, Meucci O, *et al.* The gamma-secretase-generated intracellular domain of beta-amyloid precursor protein binds Numb and inhibits Notch signaling. Proc Natl Acad Sci U S A 2002, 99: 7102–7107.

[18] Muller T, Concannon CG, Ward MW, Walsh CM, Tirniceriu AL, Tribl F, *et al.* Modulation of gene expression and cytoskeletal dynamics by the amyloid precursor protein intracellular domain (AICD). Mol Biol Cell 2007, 18: 201–210.

[19] Michl P, Knobel B, Downward J. CUTL1 is phosphorylated by protein kinase A, modulating its effects on cell proliferation and motility. J Biol Chem 2006, 281: 15138–15144.

[20] Liu Z, Zhou Z, Chen G, Bao S. A putative transcriptional elongation factor hIws1 is essential for mammalian cell proliferation. Biochem Biophys Res Commun 2007, 353: 47–53.

[21] Zhang Z, Hartmann H, Do VM, Abramowski D, Sturchler-Pierrat C, Staufenbiel M, *et al*. Destabilization of β-catenin by mutations in presenilin-1 potentiates neuronal apoptosis. Nature 1998, 395: 698–702.